The effect of crowder charge in a model polymer–colloid system for macromolecular crowding: Polymer structure and dynamics

Swomitra Palit, Lilin He, William A. Hamilton, Arun Yethiraj, and Anand Yethiraj

Citation: The Journal of Chemical Physics **147**, 114902 (2017); doi: 10.1063/1.4986353
View online: http://dx.doi.org/10.1063/1.4986353
View Table of Contents: http://aip.scitation.org/toc/jcp/147/11
Published by the American Institute of Physics

The effect of crowder charge in a model polymer–colloid system for macromolecular crowding: Polymer structure and dynamics

Swomitra Palit,[1,a)] Lilin He,[2] William A. Hamilton,[3] Arun Yethiraj,[4] and Anand Yethiraj[1,b)]
[1]*Department of Physics and Physical Oceanography, Memorial University, St. John's, Newfoundland and Labrador A1B3X7, Canada*
[2]*Biology and Soft Matter Division, Neutron Sciences Directorate, Oak Ridge National Laboratory, Oak Ridge, Tennessee 37831, USA*
[3]*Instrument and Source Division, Neutron Sciences Directorate, Oak Ridge National Laboratory, Oak Ridge, Tennessee 37831, USA*
[4]*Department of Chemistry, University of Wisconsin, Madison, Wisconsin 53706, USA*

(Received 4 June 2017; accepted 30 August 2017; published online 18 September 2017)

We have examined the effect of crowder particle charge on macromolecular structure, studied *via* small-angle neutron scattering, and translational dynamics, studied *via* pulsed-field gradient NMR, in addition to bulk viscosity measurements, in a polymer macromolecule (polyethylene glycol)—nanoparticle crowder (polysucrose, Ficoll70) model system, in the case where polymer size and crowder size are comparable. While there are modest effects of crowder charge on polymer dynamics at relatively low packing fractions, there is only a tiny effect at the high packing fractions that represent the limit of molecular crowding. We find, *via* different measures of macromolecular mobility, that the mobility of the flexible polymer in the crowding limit is 10–100 times larger than that of the compact, spherical crowder in spite of their similar size, implying that the flexible polymer chain is able to squeeze through crowder interstices. *Published by AIP Publishing.* [http://dx.doi.org/10.1063/1.4986353]

I. INTRODUCTION

The cell cytoplasm is crowded[1,2] and macromolecular crowding affects molecular transport inside living cells profoundly, with a nanoparticle soup of crowders of different sizes, shapes, hydrophobicities, and charge occupying much of the intracellular space. While much study of macromolecular crowding has focused on the (entropic) volume exclusion effect,[3–5] other (enthalpic or chemical) interactions are likely equally important: examples are charge, hydrophobicity, and hydrogen bonding.[6–9] In addition to these, solution heterogeneity and micro-viscosity has also been identified to play a big role in macromolecular crowding.[10–13] As a result, depending on the environment, macromolecules can either compact into smaller localized regions (as happens with DNA in the presence of added polymer and salt solutions[14]) or adopt more complex conformations. Thus, a careful unraveling of the effect of intermolecular interactions on macromolecular conformations and dynamics in crowded environments has been recognized to be important.[6]

The local environment plays an important role in macromolecular transport, and molecular shape has been suggested to be important: in particular Wang *et al.*[15] have shown that a disordered protein that diffuses slower than a globular protein in dilute conditions in fact exhibits 5-to-50-fold faster diffusion relative to the globular protein in a crowded environment, indicating shape-dependence of the macromolecular dynamics. Such a dramatic (relative) speed up could be important in phenomena from protein diffusion to cell signaling *in vivo*.[16–18] Addressing the question of macromolecular transport in a simple colloid-polymer system would thus enable a deeper understanding of this enhanced dynamics.

A colloidal sphere in dilute solution obeys the Stokes-Einstein (S-E) relation, which relates the molecular self-diffusion coefficient to its hydrodynamic radius and the bulk solvent viscosity. A modified S-E relation, where the self-diffusivity of the macromolecule varies inversely as the bulk suspension viscosity, remains valid even in environments where it might be expected to break down: a recent example in soft colloids finds that it is valid, surprisingly, even close to the glass transition.[19] In crowded cellular environments, however, breakdown of the modified S-E relation has been inferred *via* the observation of multiple microscopic viscosities, distinct from the bulk suspension viscosity, in a single multi-component medium.[10] While the validity of an S-E-like relationship between self-diffusivity, hydrodynamic size, and viscosity is not obvious in a heterogeneous environment, the microscopic viscosities, or alternatively, diffusion time scales $\tau = R_H^2/D$, provide a useful way to report simultaneously the change in macromolecular size and the change in macromolecular dynamics.

Experimentally disentangling the effects of changes to macromolecular size, hydrodynamic coupling between macromolecules, and direct obstructed diffusion, all of which occur simultaneously, is very challenging in nanoscale systems. In this study, we employ multiple experimental techniques to examine the effect of crowder particle charge on macromolecular structure and dynamics. Via pulsed-field-gradient (PFG)

[a)]Electronic mail: swomitra@mun.ca.
[b)]Electronic mail: ayethiraj@mun.ca.

NMR, we can obtain self-diffusivities of each chemical species in a simple model system consisting of non-ionic polymer (polyethylene glycol, PEG) and a compact, spherical polysucrose crowder (Ficoll70), both of roughly the same size, with the ratio of polymer radius of gyration R_g and crowder radius R, i.e., $\lambda = R_g/R \sim 1$.

The Ficoll70 diffusivity exhibits complex behaviour that we examine in a related work, see companion paper.[20] We obtain polymer size (R_g) in very similar samples, apart from using deuterated PEG and contrast-matched Ficoll70 solutions, by small-angle neutron scattering (SANS). The independent access to diffusivity and size allows us to examine other contributions to macromolecular dynamics: for example, in this system, the polymer and crowder have very similar hydrodynamic sizes, but the polymer is a Gaussian chain while the crowder is a compact spherical object.

In a recent study,[21] we have shown that the uncharged Ficoll70 crowder induces little compression in the polymer, consistent with a simulation that assumes hard-sphere crowders;[22] this suggests that Ficoll70 does not associate, and is thus an inert crowder, at least with respect to PEG. However, it is unclear whether an uncharged, hard-sphere crowder is relevant to real biophysical situations, such as macromolecular crowding in living cells where the macromolecules are charged entities, such as proteins and nucleic acids.

This work examines the biophysical relevance of the polysucrose crowder. We introduce charge on the crowder as a way of softening the crowder-crowder interactions *via* electrostatic repulsions, and compare polymer diffusion in charged crowders with those in bacterial cell lysates.

II. BACKGROUND

The spectral sensitivity of PFG NMR allows one to obtain dynamics of multiple species in complex systems simultaneously.[23–26] Using this spectral selectivity, we measure the self-diffusion coefficient (of both polymer and crowder) as a function of polymer concentration (c_p) and crowder packing fraction (Φ_F). For a polymer diffusing in a colloidal suspension, one may write a modified Stokes-Einstein equation,

$$D(c_p, \Phi_F) = \frac{k_B T}{6\pi \eta_\mu(c_p, \Phi_F) R_H(c_p, \Phi_F)}, \tag{1}$$

where $R_H(c_p, \Phi_F)$ is the hydrodynamic radius and $\eta_\mu(c_p, \Phi_F)$ is *an effective* microscopic viscosity that is not necessarily the same as the suspension viscosity $\eta(\Phi_F)$ (due to the low polymer concentrations, the suspension viscosity depends only on the crowder packing fraction). $\eta_\mu(c_p, \Phi_F)$ is sensitive to hydrodynamic coupling and is thus a function of c_p and Φ_F: in dilute aqueous solution ($c_p \to 0$ and $\Phi_F \to 0$), $\eta_\mu(c_p, \Phi_F)/\eta_0 \to 1$, where η_0 is the viscosity of water.

While writing D in a S-E like form is valid in the Zimm regime where $D \sim 1/R_H$, deviation of $\eta_\mu(c_p, \Phi_F)$ from the bulk suspension viscosity $\eta_{Bulk}(\Phi_F)$ signals breakdown of the S-E relation. One can, regardless, always define a characteristic time scale for a macromolecule to diffuse its own size

$$\tau = {R_H}^2/D \tag{2}$$

which also accounts for both size and diffusivity changes.

Using SANS, we measure the radius of gyration, R_g, of the deuterated polymer as a function of c_p and Φ_F in an environment where the crowder contrast has been minimized (see Sec. III and the supplementary material for details). The ratio $\alpha = R_g/R_H$, is known to be constant in the dilute regime, and its value varies from 1.2 to 1.5 as one goes from a Gaussian to a self-avoiding polymer chain. The c_p and Φ_F dependence of α is thus relatively weak, and we can replace $R_H \approx \alpha R_g$ in Eq. (1) and obtain the microscopic viscosity $\eta_\mu(c_p, \Phi_F)$ of the polymer chain: generically a decreasing function of both c_p and Φ_F. Measuring all the above quantities would allow a complete comparison to any theoretical model for the hydrodynamics of macromolecular crowding.

In previous work on polymer dynamics in the presence of uncharged crowders,[21] we discovered that the polymer self-diffusion coefficient exhibits a sharp change from a polymer-concentration independent dilute regime [with a plateau value $D(0, \Phi_F)$] to a crossover regime above a concentration $c^\star$ where $D(c_p, \Phi_F)$ could be fitted with an exponential dependence on c_p. This is expressed in the piecewise function

$$\begin{aligned} D(c_p, \Phi_F) &= D(0, \Phi_F), && c_p \le c^\star, \\ D(c_p, \Phi_F) &= D^\star(\Phi_F) \exp(-c_p/c_2), && c_p > c^\star. \end{aligned} \tag{3}$$

For each Ficoll70 packing fraction Φ_F, we obtain, in addition to $D(0, \Phi_F)$ and $c^\star$, a second characteristic concentration c_2 that describes the exponential dependence above $c^\star$. The polymer radius of gyration R_g, measured *via* SANS, was constant below a characteristic concentration $c^\star$—we refer to this value as $R_g(0, \Phi_F)$—and showing a linear dependence on polymer concentration above $c^\star$. The existence of a common polymer overlap concentration $c^\star$ to the diffusivity and size is unsurprising in pure polymer solution, but the surprise was that this persists even for finite crowder packing fraction Φ_F, and even into the crowding limit.

III. MATERIALS AND METHODS

For PFG NMR studies, we used PEG (M_w = 22 000 with M_w/M_n = 1.10), purchased from Polymer Source Inc. In SANS experiments, for contrast reasons, we used deuterated PEG (M_w = 20 000 with M_w/M_n = 1.15). Deuterated PEG was also obtained from Polymer Source Inc. Ficoll®PM 70 with average molecular weight of 70 000 (R_c = 4.5–5.5 nm) purchased from Sigma Aldrich. Deuterium Oxide (D_2O, 99.9%) was purchased from Cambridge Isotope Laboratories, Inc. Charged Ficoll (Ficoll CM 70) was a carboxymethylated derivative of Ficoll PM70, made as described in Ref. 27. It was a gift from Fissell, and was used as received after having been neutralized and dialyzed against distilled water for 4 days.

A. PFG NMR

For all samples, the desired mass of Ficoll70 was dissolved in deionized H_2O. For charged Ficoll70 solutions, the conductivity was controlled, using KCl, to a value of ≈1 mS/cm

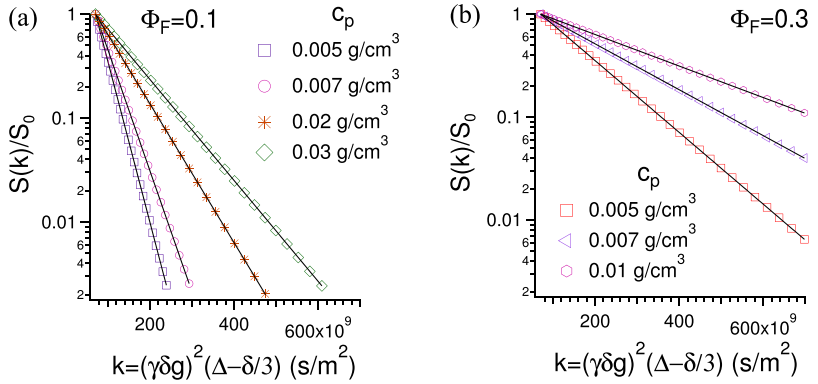

FIG. 1. The attenuation of the signal S(k)/S(0) on a log scale versus the gradient strength parameter $k = (\gamma\delta g)^2(\Delta - \delta/3)$ for PEG/charged Ficoll70 mixture of different PEG concentration: (a) $\Phi_F = 0.1$ and (b) $\Phi_F = 0.3$. All signal attenuation curves exhibit simple mono-exponential behaviour.

in order to ensure a consistent Debye-Hückel screening length for all samples. The solution was stirred for 10 h. An appropriate concentration of (undeuterated) polyethylene glycol (M_w = 22 000 with M_w/M_n = 1.10) was added to 1 cm^3 of this solution. Each time, the solution was stirred 5 h before experiment.

Samples were then transferred to 5 mm outer diameter NMR tubes. To avoid probe heating and to control sample temperature, the probe was cooled by flowing water and the temperature was maintained at 25 °C.

PFG NMR measurements were carried out on a Bruker Avance II 600 spectrometer equipped with a Bruker 14.08 T magnet and a Bruker diffusion Diff30 probe with a maximum Z gradient strength of 1800 G/cm (18 T/m). A stimulated echo pulse sequence was used to measure the diffusion coefficient. The gradient steps were varied and the signal for H_2O, PEG, and Ficoll70 were collected as a function of gradient (g). The procedure for analysis of the results is described elsewhere in detail.[26] In Fig. 1, the attenuation in PEG signal intensities were observed as a function of k $[=(\gamma\delta g)^2(\Delta - \delta/3)]$. All plots were linear for all Φ_F used in this study, which indicates that PEGs have a single diffusion component.

B. SANS

The solution preparation was identical to that for PFG NMR, with the only difference that the PEG (M_w = 20 000 with M_w/M_n = 1.15, from Polymer Source Inc.) was deuterated and the solutions were made in 60%:40% H_2O:D_2O. In order to check for consistency between NMR and SANS, one set of PFG NMR measurements were carried out in 60% H_2O/40% D_2O solutions.

For sample preparation, the desired packing fraction of Ficoll70 was dissolved in a solution of H_2O and D_2O with 40% in D_2O. The solution was stirred for 10 h. Appropriate concentration of deuterated polyethylene glycol was added to 1 cm^3 of this solution. Each time, the solution was stirred 5 h before experiment.

SANS measurements were performed at the General Purpose (GP-SANS) CG-2 instrument at Oak Ridge National Laboratory.[28] The scattered neutrons from samples were detected using a 1 m^2 area detector at two sample to detector distances of 1.7 and 18.5 m with a detector offset of 40 cm and a neutron wavelength of λ = 6 Å. This resulted in the overall q ($q = 4\pi \sin\Theta/\lambda$, where Θ is one half of the scattering angle) range of 0.004 Å^{-1}–0.5 Å^{-1}. Due to the coherent-scattering length differences[29] between hydrogen (-3.741×10^{-15} m) and deuterium (6.671×10^{-15} m), the neutron-scattering length density difference between fully hydrogenated Ficoll70 and the deuterated PEG is significant. The H_2O/D_2O composition points of minimum scattering intensity for Ficoll70 were determined using contrast variation Ficoll70 samples in solutions containing various H_2O/D_2O ratios. The ratio at which the scattering length densities of Ficoll70 and H_2O/D_2O were matched and therefore Ficoll70 did not contribute to the scattering signal was determined as (60 ± 1)% H_2O and (40 ± 1)% D_2O (see supplementary material). Therefore, only the PEG contribution appears as a q dependent intensity in the spectra regardless of Ficoll70 packing fractions.

Samples were loaded into quartz banjo cells with a thickness of 2.0 mm mounted in temperature-controlled brass sample holders and a constant temperature of 25 °C were maintained for all experiments. Data were corrected for background and empty cell contributions, and normalized to an absolute intensity using standard procedure. Scattering intensity profiles were analyzed using Igor Pro macros developed at NIST.[30] The measured neutron scattering intensity in dilute solutions per unit volume is expressed as[31]

$$I(q) = \frac{c_p\,(\Delta\rho)^2\,v_p^2}{N_a} M_w\,P(q)\,\left(1 - 2A_2\,c_p\,M_w\right), \qquad (4)$$

where c_p is the concentration in g/cm^3, M_w is the weight average molecular weight, $\Delta\rho$ is the scattering length density difference between the polymer and solvent, V_p is the volume of one polymer, and N_a is the Avogadro number. A_2 is the second virial coefficient that characterizes the average interactions between two polymers in infinitely dilute solutions, P(q) is the form factor, and P(q = 0) = 1.

The intensity as shown in Eq. (4) can be written as $I(q) = I_0\,P(q)$, where P(q) is the form factor that provides information on the size and shape of the scatterers. As shown in Fig. 2, SANS data are presented as plots of the intensity of the scattered neutron beam, I(q), as a function of scattering vector, q. For a Gaussian polymer radius of gyration R_g, the shape factor is determined by the Debye formula,[32] $P(q) = \frac{2}{x^2}\,(e^{-x} - 1 + x)$, where $x = q^2R_g^2$ and the radius of gyration of the scattering object, R_g, can be extracted from fitting the plot of I(q) vs q to the Debye model.

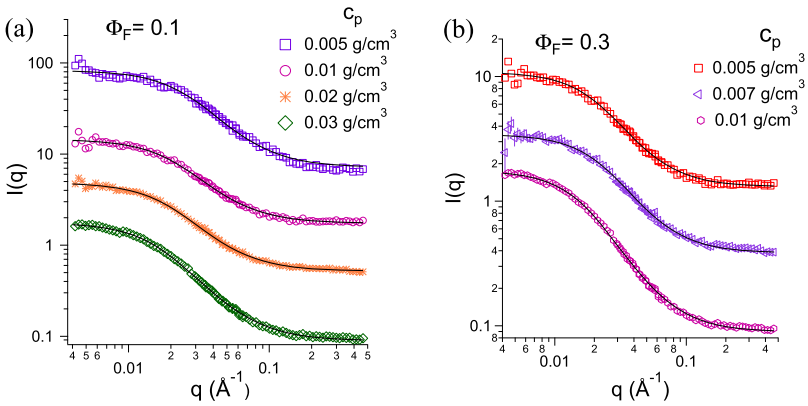

FIG. 2. SANS scattering intensity I(q) vs q for PEG/charged Ficoll70 mixture of different PEG concentration: (a) $\Phi_F = 0.1$ and (b) $\Phi_F = 0.3$. In all cases radius of gyration, R_g, of PEG, obtained from a fit to the Debye model.

C. Zeta potential

The Zeta potential (ζ) and electrophoretic mobility of Ficoll70 solutions were measured by a Zetasizer Nano Z system (Malvern Instruments Ltd, Malvern, United Kingdom). The dimensionless Zeta potential $\Psi = \zeta e/k_BT = 1.1 \pm 0.2$ and 0.21 ± 0.02 for charged and uncharged Ficoll70, respectively. The solutions of charged Ficoll70 were all prepared with added salt in order to keep the conductivity at 1 mS/cm, resulting in a Debye-Hückel screening length $\kappa^{-1} = 3.2 \pm 0.5$ nm. This corresponds to a $\kappa R_c \sim 1.4$. Given the value of the dimensionless Zeta potential Ψ and κR_c, i.e., both of order unity, electrostatics should clearly be important, but not overwhelmingly so.

D. Bulk viscosity measurement

Experiments were performed on an Anton Paar Physica MCR 301 rheometer, where the cone-plate measuring system was used to extract the flow curves. The cone-plate geometry has a diameter of 50 mm and cone angle of 0.5°. The flow curves experiments were carried out with shear rate varying from 0.001 to 100 s^{-1}.

IV. POLYMER SELF-DIFFUSIVITY IN CHARGED CROWDER

Figure 3(a) shows plots of the diffusion coefficient of PEG in aqueous suspension of charged polysucrose (charged Ficoll70, colored symbols represent diffusivities for different Ficoll70 packing fraction Φ_F). In all cases, below a critical concentration $c^\star$, which is a function of Φ_F, there is a plateau in the diffusion coefficient. This plateau is indication of the approach (with decreasing concentration) to a "polymer-dilute" regime.

Qualitatively, the existence of a polymer-dilute regime for all Φ_F for PEG self-diffusion suggests that charged Ficoll70 crowders behave similarly to uncharged crowders (which were studied previously[21]). Figure 3(b) shows $D_{PEG}(0, \Phi_F)$ as a function of Φ_F, obtained from fits of the results in Fig. 3(a) to Eq. (3). $D_{PEG}(0, \Phi_F)$ in both curves is of course identical for $\Phi_F = 0$ because there is no crowder. For $\Phi_F > 0$, $D(0, \Phi_F)$ decreases for both charged and uncharged crowders; however, the difference in $D(0, \Phi_F)$ between charged and uncharged crowders increases to a maximum near $\Phi_F = 0.15$, and then the two curves converge. The mechanisms responsible for the difference in polymer dynamics between charged and uncharged Ficoll70 is uncertain. This cannot be explained by a simple volume exclusion model of crowding. It is feasible that the structure of the cluster and void space of charged and uncharged Ficoll70 are different. A more detailed understanding of Ficoll70 structure and inter-particle interactions will be necessary in order to understand this difference; computer simulations with charged and uncharged crowders as a function of the packing fraction would be useful in this regard.

We see in Fig. 3(c) that the critical concentration $c^\star$ is very sensitive to electrostatics: as Φ_F is increased, $c^\star$ is initially 0.005 g/cm^3 at $\Phi_F = 0$, but decreases much less rapidly for charged Ficoll70 than for uncharged Ficoll70.

However, the two decreases converge for larger Φ_F, with $c^\star \sim 0.015$ g/cm^3 for $\Phi_F = 0.3$. For polymer solutions, one normally expects $c^\star(0) \sim N/R_g^3$ (where N is the number of monomers). Therefore, in the presence of a crowder, if one expects the "internal concentration" $c^\star(0)$ to be constant, then we would expect $c^\star(\Phi_F) = c^\star(0)(1 - \Phi_F)$ [solid blue line in Fig. 3(c)]. Instead, one sees roughly linear behavior at low Φ_F with $c^\star(\Phi_F) = c^\star(0)(1 - \beta_1\Phi_F)$, where $\beta_1 = 10 \pm 3$ for uncharged Ficoll70 and 3.0±0.2 for anionic Ficoll70. This suggests that even if the picture above is correct, the effective free volume is reduced much more than expected, but this reduction is much smaller for anionic Ficoll70, where one would expect less self-clustering.

Above $c^\star$, the story is different. The exponential dependence of $D(c_p, \Phi_F)$ on polymer concentration c_p yields a *second* characteristic concentration, c_2, shown in Fig. 3(d), which decreases from $c_2 = 0.0345$ g/cm^3 to $c_2 = 0.005$ g/cm^3: note that this behavior is identical for charged and uncharged crowders, suggesting that while the diffusivity at infinite polymer dilution depends on crowder charge, its dependence on polymer concentration is independent of crowder charge. We can use the fitted results to recast all the measurements of polymer self-diffusion in charged Ficoll70 (colored symbols), as well as the previous results with uncharged Ficoll70[21] (gray symbols), plotting a dimensionless quantity $Y = (c_2/c^\star)\ln(D(c_p, \Phi_F)/D^\star)$ as a function of a scaled polymer concentration $X = c_p/c^\star$. Agreement with Eq. (3) would require $Y = -1$ when $X \leq 1$, and $Y = -X$, otherwise. Clearly, all the results (for polymer dynamics in both charged and uncharged crowders) obey this behaviour. Moreover, the sharp transition in the dynamics that separates the dilute and the crossover regime is valid, regardless of the degrees of crowding, or the crowder charge.

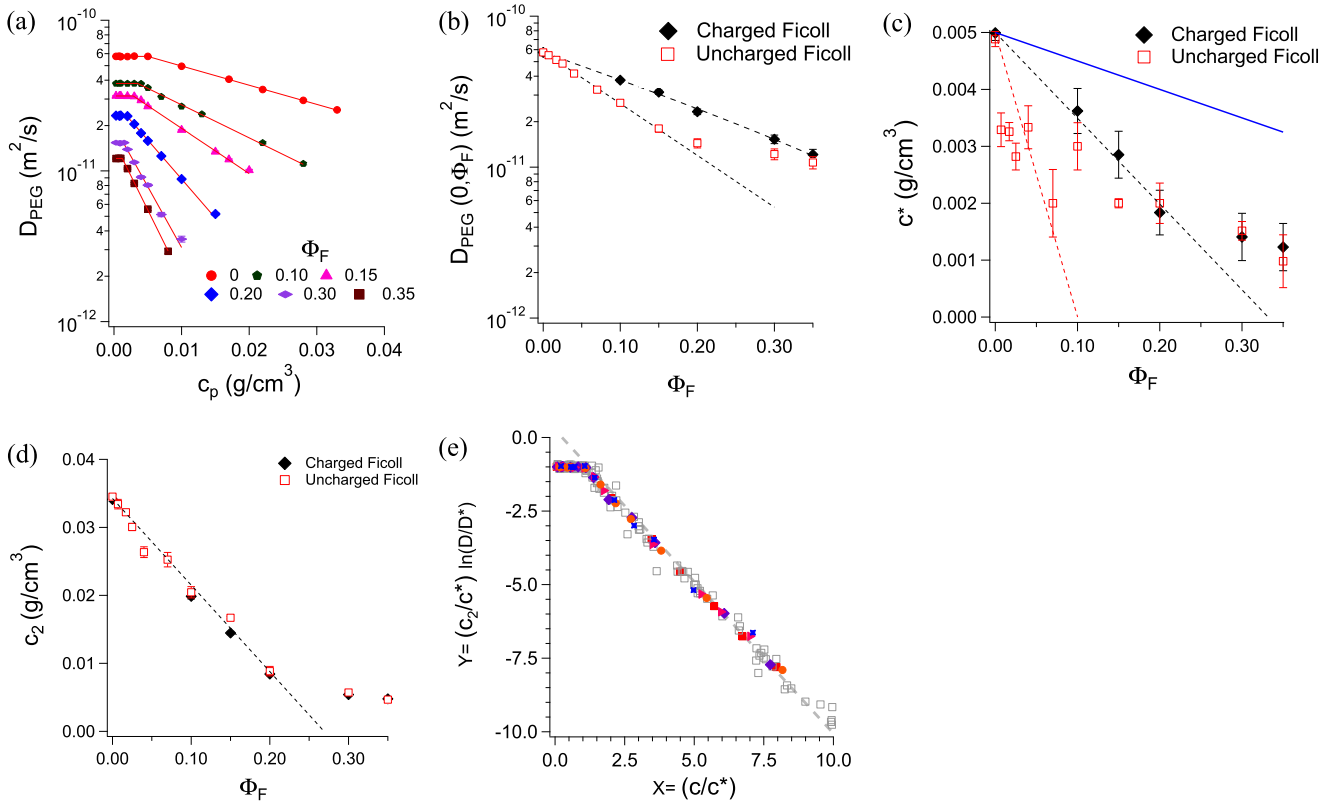

FIG. 3. Polymer dynamics in charged crowder: (a) Self-diffusion coefficient of PEG (M_w = 20 000) polymer in water as a function of polymer concentration c_p, and for several packing fractions Φ_F of charged (color, filled symbols) Ficoll70. Each dependency is fit to Eq. (3) to obtain $D(0,\Phi_F)$, and the characteristic concentrations $c^\star$ and c_2. (b) For each Ficoll70 packing fraction, a plateau in the self-diffusion coefficient, $D(0,\Phi_F)$, obtained *via* fits to the concentration dependence, is observed below a characteristic PEG concentration $c^\star$, indicating the existence of a "polymer-dilute" regime at all Φ_F. (c) For *every* crowder packing fraction, there is a characteristic PEG concentration $c^\star$, below which the diffusion coefficient is unchanging. The value of $c^\star$ shows a very different dependence on packing fraction Φ_F for uncharged and charged Ficoll70; however, it converges near $\Phi_F = 0.3$. (d) Above $c^\star$, the diffusion coefficient shows an exponential decrease; this yields a *second* characteristic PEG concentration c_2 as a function of uncharged and charged Ficoll70 packing fractions Φ_F. (e) Using the values $D^\star$, $c^\star$, and c_2 from each fit, *all* the diffusion results (as a function of c_p and Φ_F) are replotted in dimensionless form, $Y = (c_2/c^\star)\ln(D(c_p,\Phi_F)/D^\star)$ as a function of a scaled polymer concentration $X = c_p/c^\star$. There is good collapse onto one master plot that shows a sharp transition at $X = 1$ from a polymer-dilute plateau to an exponential concentration dependence of the diffusion coefficient. The results for uncharged Ficoll70 are shown in gray.

As discussed in Sec. II and in previous work in the presence of an uncharged crowder,[21] such an exponential relationship could be consistent with the theory for atomic liquids where an exponential relationship between atomic diffusion and the excess entropy is predicted.[33,34] Such a remarkably universal exponential dependence at all Φ_F, and independent of crowder charge, suggests that above $c^\star$, only the structure is important, and colloidal hydrodynamics is unimportant. One should also be able to examine the Φ_F dependence of c_2 further. Up to $\Phi_F = 0.2$, one can fit the dependence to $c_2(\Phi_F) = c_2(0)(1 - \beta_2\Phi_F)$, with $\beta_2 = 3.8 \pm 0.2$ for both uncharged and anionic Ficoll70. This suggests, interestingly, that the effective free volume above the polymer overlap concentration is insensitive to crowder structure, and decreases proportionally with increasing Φ_F. The reason for the observed value of β_1 and β_2 is not known. However, it is noted that there is a relationship between c_2 and the polymer concentration, c_{ps}, where phase separation is first observed in the PEG-Ficoll system (see supplementary material). Indeed, the ratio c_2/c_{ps}, at a given Φ_F, depends neither on polymer molecular weight M_w nor on crowder charge, suggesting that it is related in some way to polymer-polymer association.

Whether high concentrations of inert synthetic crowders can faithfully mimic cytosolic conditions is an important question. One could ask "What is the relevance to cellular environments of the dynamics of a polymer chain in charged and uncharged colloidal crowders?" The cellular environment is composed of macromolecules of different shape and size (entropy) with, additionally, electrostatic and chemical interactions of all macromolecules (enthalpy). Bacterial cell lysates are physiologically more relevant and more closely mimic the soft interactions of the cytosol, but it was unclear *a priori* if macromolecular dynamics is even qualitatively similar to model crowders. What the above shows is that macromolecular dynamics in cell lysates is indeed, qualitatively and at least semi-quantitatively, comparable to model crowders.

In Fig. 4, we make a first attempt at addressing this question by comparing polymer self-diffusion coefficients at $\Phi_F = 0.1$, for PEG (as a function of polymer concentration c_p) for charged Ficoll70, uncharged Ficoll70, and a bacterial cell lysate solution. The bacterial cell lysate solution is prepared at a concentration of 13.7 g/cm^3 which corresponds to a packing fraction of 0.1, chosen because there is much more quantitative difference in diffusivities between uncharged and charged crowders at $\Phi_F = 0.1$ than in the crowding limit. The polymer

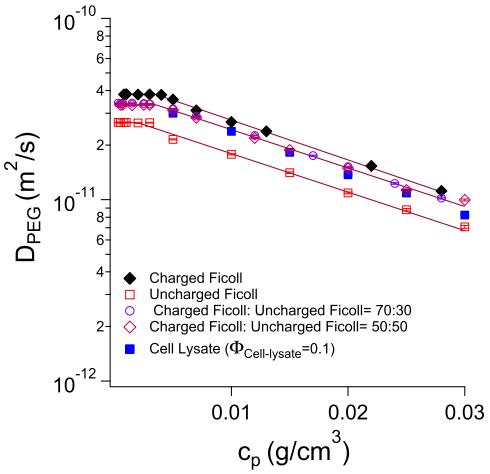

FIG. 4. Comparison of polymer diffusion in bacterial cell lysate and Ficoll70: The self-diffusion coefficient of PEG in bacterial cell lysate lies in between the corresponding values in charged and uncharged crowders (at comparable packing fractions, $\Phi = 0.1$): a good match is found to a 50:50 mixture of charged and uncharged crowders.

self-diffusivity in the bacterial cell lysate shows the same exponential dependence as a function of polymer concentration. In addition, the polymer self-diffusivity in bacterial cell lysate lies in between the charged and uncharged crowders. Indeed, shown in Fig. 4, PEG diffusion in bacterial cell lysate is quantitatively close to PEG diffusion in 70:30 and 50:50 mixtures of charged and uncharged Ficoll70. This suggests that once one controls for crowder charge, macromolecular diffusion in an artificial crowder might be meaningful in biologically relevant systems.

V. QUANTIFYING THE EFFECT OF CROWDER CHARGE

In Fig. 5(a), the polymer radius of gyration R_g, obtained from SANS, is plotted as a function of c_p, for different charged Ficoll70 packing fractions Φ_F. For each Φ_F, the polymer-concentration dependence is linear and actually shows an *increase* above $\Phi_F = 0.15$. The expansion in polymer size is most likely due to the formation of clusters of polymers, a phenomenon that is known for aqueous solution of PEG without crowder.[35]

One can linearly extrapolate the radius of gyration $R_g(c_p, \Phi_F)$ [in Fig. 5(a)] to $c^\star$. This yields [Fig. 5(b)] the polymer size in the polymer-dilute regime: $R_g(0, \Phi_F)$. For uncharged crowders, results from previous work[21] show a weak dependence on Φ_F. For charged crowders, there is

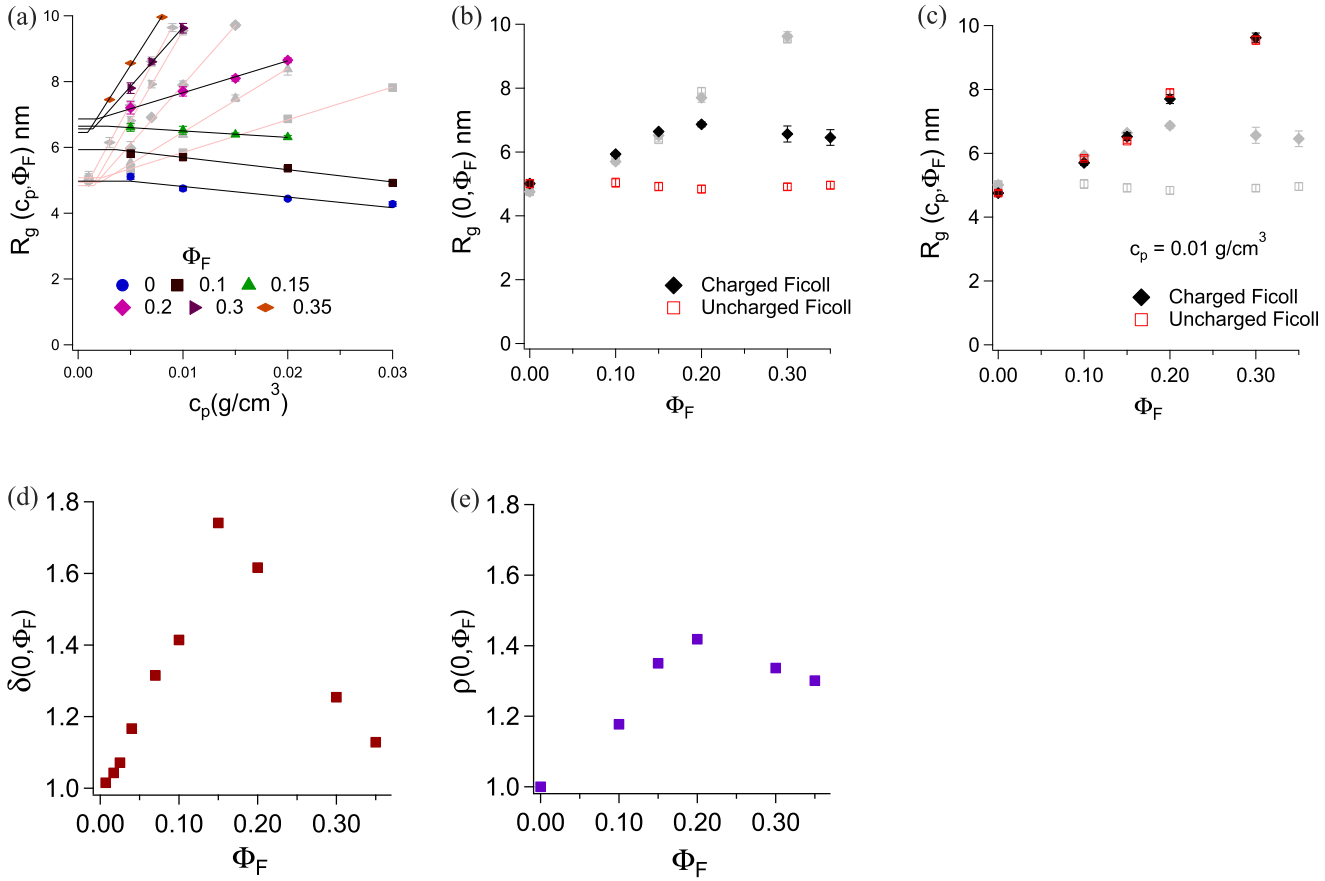

FIG. 5. The effect of crowder charge: (a) Radius of gyration $R_g(c_p, \Phi_F)$ in the crossover regime shows a linear dependence with c_p at each Φ_F. In gray symbols, $R_g(c_p, \Phi_F)$ for uncharged crowders (data from Ref. 21) is shown for comparison. A linear extrapolation of the radius of gyration $R_g(c_p, \Phi_F)$ to $c^\star$ yields the polymer size in the polymer-dilute regime: $R_g(0, \Phi_F)$. (b) A linear extrapolation of the radius of gyration $R_g(c_p, \Phi_F)$ to $c^\star$ yields the polymer size in the polymer-dilute regime: $R_g(0, \Phi_F)$. (c) Above $c^\star$, the radius of gyration $R_g(c_p, \Phi_F)$ for uncharged crowder is plotted as a function of Φ_F. In (b) and (c), the $c_p = 0.01$ g/cm^3 and $c_p = 0$ results are shown in gray to aid comparison. (d) Ratio of self-diffusion coefficients $\delta(0, \Phi_F) = D^{charged}(0, \Phi_F)/D^{uncharged}(0, \Phi_F)$ has a maximum value of 1.75 at $\Phi_F = 0.15$ and then decreases to ~1.1 at $\Phi_F = 0.35$. (e) The ratio of $R_g(0, \Phi_F)$ of PEG in charged and uncharged Ficoll70, $\rho(0, \Phi_F) = R_g^{charged}(0, \Phi_F)/R_g^{uncharged}(0, \Phi_F)$ increases to a maximum value of 1.4, and then decreases to 1.3 in the crowding limit, i.e., at $\Phi_F = 0.35$.

a ≈ 30%–40% increase in R_g in both cases, which is significant. Above the overlap concentration, $c^\star$, the radius of gyration $R_g(c_p, \Phi_F)$, for $c_p = 0.01$ g/cm^3, is plotted as a function of Φ_F [Fig. 5(c)]. Here, there is a steady and significant increase of R_g, attributed to polymer-polymer clustering. This increase is insensitive to the crowder charge.

VI. ENHANCED MICRO-SCALE MOBILITIES

Figure 5(d) shows the Φ_F dependence of the *ratio* $\rho(0, \Phi_F) = R_g^{charged}(0, \Phi_F)/R_g^{uncharged}(0, \Phi_F)$, which compares polymer size in charged versus uncharged Ficoll70. PEG *in the dilute limit* is relatively unchanged when the crowder is uncharged. There is evidence from previous work[21] that the size of isolated PEG chains in PEG-Ficoll70 suspensions agrees quantitatively with simulation, indicating that Ficoll70 is an inert crowder for PEG. For charged crowders, however, PEG expands by a factor of 1.35 at $\Phi_F = 0.15$ and 1.3 at $\Phi_F = 0.35$.

From Fig. 3, we can also calculate the ratio $\delta = D^{charged}/D^{uncharged}$ (in the polymer-dilute limit) as a function of Φ_F, shown in Fig. 5(e), which increases from unity at Φ_F = 0–1.75 at $\Phi_F = 0.15$, but decreases back to 1.1 at $\Phi_F = 0.35$. Hence, in the crowding limit, the polymer dynamics is nearly unaffected by crowder charge in spite of the size [shown in Fig. 5(d)] increasing modestly by 30% of its value in dilute solution. Above the polymer concentration $c^\star$, how polymer chains *interact with other polymer chains* is also not sensitive to the charge of the crowder, and exhibits universal exponential behaviour. This is seen both in the structure [Fig. 5(c), colored symbols] and in the dynamics [Fig. 3(e)]. A precise understanding of the behavior in this regime would require unraveling polymer-polymer clustering and the structure of the free volume, and will be the focus of future work where we can examine the structure of the crowder *via* SANS.

We do not know the reason either for the expansion of R_g in the presence of a charged crowder or the enhancement of self-diffusion in the presence of a charged crowder. Polymer-crowder interaction is unlikely since PEG is uncharged, so it must indirectly be the result of Ficoll-Ficoll interactions. While examining Ficoll70 structure *via* SANS requires extensive experiments with deuterated Ficoll, crowder dynamics is accessible directly from PFG NMR experiments, and is discussed in a companion paper.[20]

We are finally ready to examine the macromolecular environments for polymer and crowder, by looking at the relative polymer self-diffusivities, time scales, and micro-viscosities.

Using Eq. (1), and the diffusion coefficient D(0, 0) (from PFG NMR) and $R_g(0, 0)$ (from SANS) of an isolated polymer in the presence of crowder, and setting $\eta_\mu(0, 0) \equiv \eta_0$, we obtain $R_g/R_H = 1.18$. This may be compared with the theoretical and experimental values of 1.24 and 1.16, respectively (for a θ solvent),[36] as tabulated by Oono and Kohmoto.[36]

In a companion work,[20] we find that Ficoll70 solutions form clusters above a characteristic Φ_F (0.05 for uncharged and 0.1 for charged Ficoll70). In addition, we obtain the fraction of cluster $f_{cluster}$ and the fraction of monomer $1 - f_{cluster}$, for a range of Φ_F, and the diffusivities $D_{cluster}$ and $D_{monomer}$ of both cluster and monomer species.

Figure 6(a) shows the ratio of polymer to crowder self-diffusivity, $D_{PEG}(0, \Phi_F)/D^{eff}_{Ficoll}(\Phi_F)$, as a function of Φ_F. Since the Ficoll70 forms clusters, D^{eff}_{Ficoll} is obtained by a weighted average $D^{eff}_{Ficoll} = f_{cluster}D_{cluster} + (1 - f_{cluster})D_{monomer}$. All the quantities in this weighted average are measured [Figs. 3(a), 3(b), and 4(b) in the companion article.[20]] PEG dynamics is enhanced sharply (by a factor of 10–100 with respect to Ficoll70 dynamics, in uncharged and charged crowders) as Φ_F approached the crowding limit. Denoting τ as the time scale for a macromolecule to diffuse its own radius [Eq. (2)], the ratio $\tau_{PEG}(0, \Phi_F)/\tau_{Ficoll}(\Phi_F)$ [Fig. 6(b)] shows a concomitant decrease by 1–2 orders of magnitude with increasing Φ_F.

Finally, we plot the *relative* polymer microscale viscosity $\eta_\mu(0, \Phi)/\eta_0$ against its bulk equivalent $\eta(\Phi)/\eta_0$ [Fig. 6(d)], using the Ficoll70 suspension viscosity measured using a cone-plate rheometer to obtain both the viscosity of water η_0, and the viscosity of the suspension as a function of Φ, $\eta(\Phi)$ (see Sec. III). At $\Phi_F = 0$, $\eta_\mu^{PEG}(0, \Phi_F)/\eta_0 = 1$. As Φ_F increases

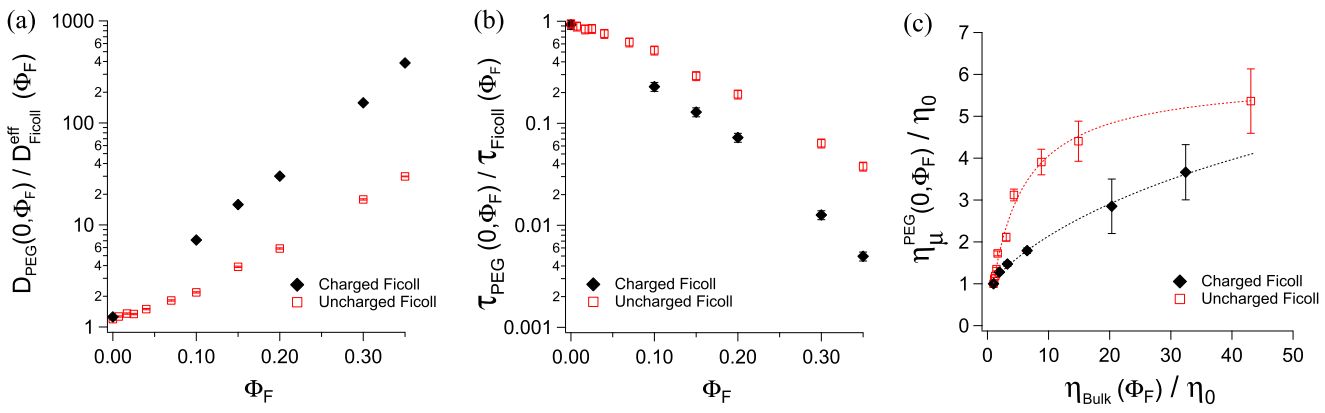

FIG. 6. Enhanced micro-scale mobilities: (a) Comparison of the diffusivity ratio $D_{PEG}(0, \Phi_F)/D^{eff}_{Ficoll}(\Phi_F)$ for charged and uncharged Ficoll70 as a function of Φ_F shows a significant (10–100 fold) enhancement of the polymer (PEG) dynamics, relative to the compact (Ficoll70) crowder. (b) The ratio of characteristic time scale τ_{PEG}/τ_{Ficoll} concomitantly *decreases* by 1–2 orders of magnitude as a function of Φ_F. (c) Relative micro-scale viscosity of PEG, $\eta_\mu^{PEG}(0, \Phi_F)/\eta_0$, obtained from $D(0, \Phi_F)$ and $R_g(0, \Phi_F)$ as a function of uncharged and charged relative Ficoll70 viscosity $\eta_{Bulk}(\Phi_F)/\eta_0$. The broken curves may be treated as a guide to the eye.

to $\Phi_F = 0.3$, $\eta_\mu^{PEG}(0, \Phi_F)/\eta_0$ increases only by a factor of ≈4, while $\eta_{Bulk}(\Phi_F)/\eta_0$ increases by a factor of 30-40; the micro-viscosity is thus approximately 10 times smaller than the bulk viscosity in the limit of crowding.

Fluorescence correlation spectroscopy (FCS) has been used to obtain the micro-viscosity via diffusion of a probe molecule (protein) in the presence of a macromolecular crowder (Ficoll70). According to these studies, depending on the size of the protein, the micro-viscosity of Ficoll70 is found 4–7 times larger than the viscosity of pure water.[11,37] Other studies have also reported diffusion coefficients of proteins that suggest a difference between micro-viscosity and bulk viscosity.[38,39] Rashid *et al.*[13] have reported that the micro-viscosity experienced by a fluorescent probe molecule in Ficoll70 is up to 8 times smaller than the bulk viscosity in the limit of crowding, roughly consistent with our findings.

By all measures, two macromolecules of *similar nanometric size* have very different mobilities. The flexible linear polymer, which has access to chainlike dynamical modes (such as reptation) is 10–100 times more mobile than the more compact crowder.

VII. DISCUSSION AND CONCLUSION

In this work, we examine the role of crowder charge on macromolecular dynamics, with no other parameters changing.

A. Charge has a weak effect on crowding

At $\Phi_F = 0.35$, crowder charge only barely affects dynamics. The ratio $\delta(0, \Phi_F)$ of polymer diffusivity (for charged versus uncharged crowder), while large at $\Phi_F = 0.15$, is only ∼1.1 in the crowding limit.

B. Ficoll70 has biophysical relevance in crowding

While Ficoll70 is not a simple crowder, its use as a crowder might nevertheless have biophysical relevance. The concentration dependence of polymer self-diffusivity in charged and uncharged Ficoll70 appear to be upper and lower bounds for the self-diffusivity in a more biologically relevant cell lysate solution at the same concentration! We find that we can construct an artificial crowder that mimics polymer dynamics in cell lysate by making an appropriate mixture of charged and uncharged crowders.

C. Flexibility aids macromolecular transport

A comparison between the polymer self-diffusivity and diffusion time scales with that of the compact crowder (and a polymer micro-viscosity with the bulk suspension viscosity) suggests that the microscopic dynamics of the polymer is significantly enhanced in the crowding limit relative to the expectations for a homogenous solution of the same bulk viscosity. In particular, the polymer (PEG) has a mobility that is 10–100 times larger than the compact, Ficoll70 crowder. Wang *et al.*[15] have indicated that macromolecular shape might be a key parameter in protein diffusion in the presence of macromolecular crowding. The current work implies, in a simple model system for crowding, that *flexibility* (i.e., the changing transient shape) makes a diffusing chainlike macromolecule very different from a diffusing colloid and affects its mobility profoundly.

It is, of course, possible that it is not the polymer dynamics that is enhanced, but that the crowder hydrodynamic size is enhanced due to factors such as hydrogen bonding. Having measured Ficoll70 cluster size [Fig. 4(a) in the companion article,[20] $R_{cluster}/R_{monomer} < 3$], this would account for only a small enhancement, not the 10–100 fold enhancement seen.

The long time goal of tandem PFG NMR and SANS studies of crowding is to study charged polymers or proteins in a charged crowder. In addition, examining the role of flexibility (e.g., comparing disordered proteins with globular proteins) is of interest. The current work represents an important step towards that goal.

SUPPLEMENTARY MATERIAL

See Supplementary Material for results that aid in the physical interpretation of second characteristic concentration (c_2), a plot of the optimum contrast matching to wipe out the contribution of Ficoll70 in scattering intensity, and comparison of R_g obtained from Debye and Guinier fits.

ACKNOWLEDGMENTS

This work was supported by the Natural Sciences and Engineering Research Council of Canada. A portion of this research used resources at the High Flux Isotope Reactor, a DOE Office of Science User Facility operated by the Oak Ridge National Laboratory. We thank William Fissell for generously providing us with charged Ficoll70, and John Bechhoefer, Jure Dobnikar, and Stefan Wallin for the useful discussions. We are also grateful to Valerie Booth and Donna Jackman for providing us with the cell lysate, as well as for DLS characterizations of Ficoll70.

[1] A. B. Fulton, Cell **30**, 345 (1982).
[2] R. J. Ellis, Trends Biochem. Sci. **26**, 597 (2001).
[3] A. P. Minton, Biopolymers **20**, 2093 (1981).
[4] S. B. Zimmerman and A. P. Minton, Annu. Rev. Biophys. Biomol. Struct. **22**, 27 (1993).
[5] A. P. Minton, Curr. Opin. Biotechnol. **8**, 65 (1997).
[6] H. X. Zhou, G. Rivas, and A. P. Minton, Annu. Rev. Biophys. **37**, 375 (2008).
[7] Y. Wang, M. Sarkar, A. E. Smith, A. S. Krois, and G. J. Pielak, J. Am. Chem. Soc. **134**, 16614 (2012).
[8] A. C. Miklos, M. Sarkar, Y. Wang, and G. J. Pielak, J. Am. Chem. Soc. **133**, 7116 (2011).
[9] M. Sarkar, A. E. Smith, and G. J. Pielak, Proc. Natl. Acad. Sci. U. S. A. **110**, 19342 (2013).
[10] A. B. Goins, H. Sanabria, and M. N. Waxham, Biophys. J. **95**, 5362 (2008).
[11] S. Mukherjee, M. M. Waegele, P. Chowdhury, L. Guo, and F. Gai, J. Mol. Biol. **393**, 227 (2009).
[12] I. M. Kuznetsova, B. Y. Zaslavsky, L. Breydo, K. K. Turoverov, and V. N. Uversky, Molecules **20**, 1377 (2015).
[13] R. Rashid, S. M. L. Chee, M. Raghunath, and T. Wohland, Phys. Biol. **12**, 034001 (2015).
[14] L. S. Lerman, Proc. Natl. Acad. Sci. U. S. A. **68**, 1886 (1971).
[15] Y. Wang, L. A. Benton, V. Singh, and G. J. Pielak, J. Phys. Chem. Lett. **3**, 2703 (2012).
[16] M. C. Konopka, I. A. Shkel, S. Cayley, M. T. Record, and J. C. Weisshaar, J. Bacteriol. **188**, 6115 (2006).
[17] Y. Phillip and G. Schreiber, FEBS Lett. **587**, 1046 (2013).
[18] L. M. Iakoucheva, C. J. Brown, J. D. Lawson, Z. Obradović, and A. K. Dunker, J. Mol. Biol. **323**, 573 (2002).

[19]S. Gupta, J. Stellbrink, E. Zaccarelli, C. N. Likos, M. Camargo, P. Holmqvist, J. Allgaier, L. Willner, and D. Richter, Phys. Rev. Lett. **115**, 128302 (2015).
[20]S. Palit and A. Yethiraj, J. Chem. Phys. **147**, 074901 (2017).
[21]S. Palit, L. He, W. A. Hamilton, A. Yethiraj, and A. Yethiraj, Phys. Rev. Lett. **118**, 097801 (2017).
[22]H. Kang, P. A. Pincus, C. Hyeon, and D. Thirumalai, Phys. Rev. Lett. **114**, 068303 (2015).
[23]O. Söderman and P. Stilbs, Prog. Nucl. Magn. Reson. Spectrosc. **26**, 445 (1994).
[24]K. I. Momot and P. W. Kuchel, Concepts Magn. Reson., Part A **28A**, 249 (2006).
[25]T. Stait-Gardner, S. A. Willis, N. N. Yadav, G. Zheng, and W. S. Price, Diffus. Fundam. **11**, 15 (2009), http://nbn-resolving.de/urn:nbn:de:bsz:15-qucosa-189360.
[26]S. Barhoum, S. Palit, and A. Yethiraj, Prog. Nucl. Magn. Reson. Spectrosc. **94-95**, 1 (2016).
[27]J. Groszek, L. Li, N. Ferrell, R. Smith, C. A. Zorman, C. L. Hofmann, S. Roy, and W. H. Fissell, Am. J. Physiol.: Renal Physiol. **299**, F752 (2010).
[28]G. D. Wignall, K. C. Littrell, W. T. Heller, Y. B. Melnichenko, K. M. Bailey, G. W. Lynn, D. A. Myles, V. S. Urban, M. V. Buchanan, D. L. Selby, and P. D. Butler, J. Appl. Crystallogr. **45**, 990 (2012).
[29]Y. B. Melnichenko and G. D. Wignall, J. Appl. Phys. **102**, 021101 (2007).
[30]S. R. Kline, J. Appl. Crystallogr. **39**, 895 (2006).
[31]G. D. Wignall and Y. B. Melnichenko, Rep. Prog. Phys. **68**, 1761 (2005).
[32]P. Debye, J. Appl. Phys. **15**, 338 (1944).
[33]Y. Rosenfeld, Phys. Rev. A **15**, 2545 (1977).
[34]M. Dzugutov, Nature **381**, 137 (1996).
[35]B. Hammouda, D. Ho, and S. Kline, Macromolecules **35**, 8578 (2002).
[36]Y. Oono and M. Kohmoto, J. Chem. Phys. **78**, 520 (1983).
[37]S. Patra, N. Erwin, and R. Winter, ChemPhysChem **17**, 2164 (2016).
[38]D. Lavalette, C. Tétreau, M. Tourbez, and Y. Blouquit, Biophys. J. **76**, 2744 (1999).
[39]N. A. Busch, T. Kim, and V. A. Bloomfield, Macromolecules **33**, 5932 (2000).